Growth of Monolayer MoS$_2$ on Hydrophobic Substrates as a Novel and Feasible Method to Prevent the Ambient Degradation of Monolayer MoS$_2$

Kevin Yao, Dave Banerjee, John D. Femi-Oyetoro, Evan Hathaway, Yan Jiang, Brian Squires, Daniel C. Jones, Arup Neogi, Jingbiao Cui, Usha Philipose, Aryan Agarwal, Ernest Lu, Steven Yao, Mihir Khare, Ibikunle A. Ojo, Gage Marshall, and Jose Perez

Department of Physics, University of North Texas, Denton, TX 76203, United States

Monolayer (ML) molybdenum disulfide (MoS$_2$) is a novel 2-dimensional (2D) semiconductor whose properties have many applications in devices. Despite its potential, ML MoS$_2$ is limited in its use due to its degradation under exposure to ambient air. Therefore, studies of possible degradation prevention methods are important. It is well established that air humidity plays a major role in the degradation. In this paper, we investigate the effects of substrate hydrophobicity on the degradation of chemical vapor deposition (CVD) grown ML MoS$_2$. We use optical microscopy, atomic force microscopy (AFM), and Raman mapping to investigate the degradation of ML MoS$_2$ grown on SiO$_2$ and Si$_3$N$_4$ that are hydrophilic and hydrophobic substrates, respectively. Our results show that the degradation of ML MoS$_2$ on Si$_3$N$_4$ is significantly less than the degradation on SiO$_2$. These results show that using hydrophobic substrates to grow 2D transition metal dichalcogenide ML materials may diminish ambient degradation and enable improved protocols for device manufacturing.

INTRODUCTION:

In recent years, 2-dimensional transition metal dichalcogenides (2D TMDs) have been studied extensively for applications in next-generation electronics and optoelectronics [1]. Specifically, monolayer (ML) MoS$_2$, a 2D TMD, is of special interest due to its direct band gap and large spin-orbit coupling [1]. However, there have been

numerous studies that show that these materials degrade after about a year of ambient air exposure at room temperature (RT) [2-7], which may be a large impediment to their realization in practical applications. Ambient air degradation affects most 2D materials [8], so it is of interest to determine feasible methods of degradation prevention. In the case of MoS_2, reports have shown that sulfur vacancies in the films and water vapor in the air play important roles in the degradation [2-7]. In addition, it has been reported that the degradation of MoS_2 is a photo-induced effect, since degradation is not observed in samples that are kept in the dark [4]. Photoinduced degradation in the presence of water vapor and oxygen has also been reported for black phosphorus (BP) [9]. For MoS_2 and BP, the role of humidity in the degradation is believed to involve the liquefication of oxides that leaves the layer unprotected and susceptible to additional oxidation [6]. We have previously reported that degradation of ML MoS_2 proceeds by the formation of dendrites with a fractal dimension close to that of diffusion limited aggregation, indicating that the diffusion of water molecules on the MoS_2 ML is likely involved in the degradation mechanism [7]. The water molecules may be getting onto the ML MoS_2 mainly from the substrate or the ambient air. Thus, it is of interest to investigate the effects of substrate hydrophobicity on the degradation. In this paper, we investigate the degradation of CVD-grown ML MoS_2 on SiO_2 and Si_3N_4 substrates, which are hydrophilic and hydrophobic, respectively. We use optical microscopy, atomic force microscopy (AFM) and Raman mapping to investigate the degradation. We also utilize a method we have previously reported to accelerate the degradation of ML MoS_2, so that we can study the degradation process in a time frame of weeks rather than a year. This method consists of first heating the samples in air prior to leaving the samples in ambient conditions at RT [7].

We note that the most common methods currently used to prevent degradation involve encapsulating the samples with inert materials such as hexagonal boron nitride (hBN) and polymers [2] or by using vacuum storage protocols [5]. However, these methods of passivation can affect sample properties and are generally not scalable [2]. Thus, our goal is to explore the growth of MoS_2 on hydrophobic substrates as an alternative method of diminishing and preventing degradation that is more feasible for practical applications.

EXPERIMENTAL DETAILS:

The MoS_2 MLs were grown on SiO_2 and Si_3N_4 substrates using the method described in Ref. [10]. The SiO_2 substrates were 300nm SiO_2 films thermally grown on 500 μm thick degenerately doped Si wafers. The Si_3N_4 substrates were 100 nm thick Si_3N_4 films grown using plasma-enhanced CVD on degenerately doped Si wafers. The Si_3N_4 substrates were purchased from MTI Corporation [11]. Before putting the substrates in the oven, a promoter was made by dissolving 1 mg of NaCl (≥99.5%) in 1 mL of ammonium hydroxide (28% NH_3 in H_2O) with sonication for 10 minutes. The promoter was spun coated over the substrates at 3000 rpm for 60 s. The tube furnace was annealed at 900 $^\circ$C for 2 h under air flow for the purpose of cleaning the tube. After the tube furnace cooled to RT, the substrates and crucibles containing S and MoO_3 were placed in the tube. The tube was then flushed with 500 sccm of ultrahigh purity Ar gas at atmospheric pressure and RT for 10 minutes. The Ar flow was then reduced to 100 sccm, and the temperature ramped at a rate of 25 °C/minute to a growth temperature of 800°C for 20 minutes.
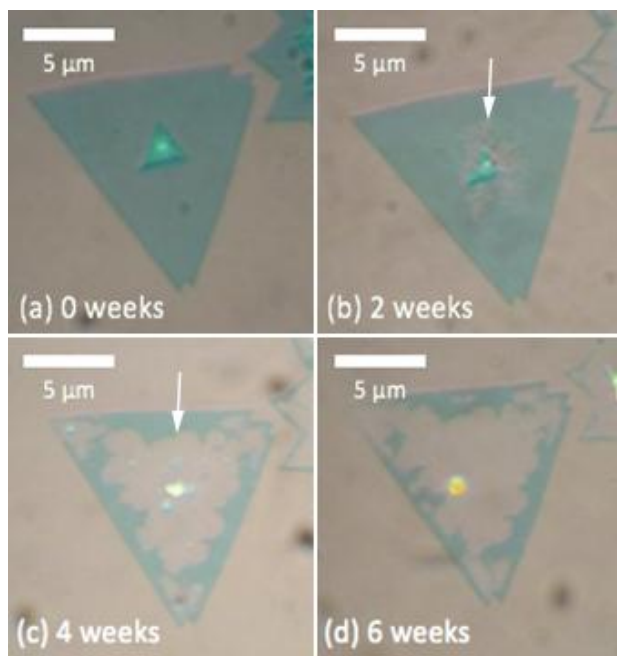
Figure 1. (a) Optical image of a CVD-grown MoS_2 ML on SiO_2 grown approximately three months prior and before exposure to ambient air at 100% RH. (b) Optical image of the sample 2 weeks after exposure to 100% RH. (c) Optical image of the sample 4 weeks after exposure to 100% RH. (d) Optical image of the sample 6 weeks after exposure to 100% RH.

The degradation acceleration method we used is described in detail in Ref. [7]. In summary, we pre-heat the samples at temperatures of 285 and 300 ºC in a tube furnace in air at atmospheric pressure for 2 h. All samples were pre-heated in the same tube furnace that had a light intensity of about 10 Lux inside when it was at RT. During pre-heating, etching of the grain boundaries occurs, creating a trench in the MoS_2 that can be observed as a lower elevation in the AFM images. The higher the pre-heating temperature, the faster the etch rate, as reported in Ref. [15], and thus the wider the etched trench. The resulting accelerated degradation is like natural degradation but takes place on a much shorter time frame [7]. This degradation process oxidizes MoS_2 into elevated dendrites that can be observed in AFM images. We note that this degradation process is distinct from the etching process. The AFM images were collected using an Ambios Q-Scope in tapping mode. Raman spectroscopy maps were obtained using a Renishaw inVia Raman Microscope with a 532 nm laser, stage step size of 0.5 µm, laser spot of 764 nm, and a spectral resolution of 1 cm^{-1}.

DISCUSSION

We first investigated the role of humidity in the degradation. Specifically, we sought to determine if a RH of 40-50% that is typical for ambient air in a building is a limiting factor in the degradation. To do this, we exposed as-grown samples to ambient air at 100% RH and RT, instead of 40-50% RH as in previous reports [2-7]. For this exposure, the samples were placed under a room light intensity of about 1000 Lux that is typical of ambient lighting in an ordinary room. We did not pre-heat this sample to accelerate degradation because we aimed to compare how an increase in RH would affect degradation without the addition of another variable. Figure 1 (a) is an optical image that shows a MoS_2 ML sample grown approximately three months prior on SiO_2 and before exposure to ambient air at 100% RH and RT. The interior of the sample appears homogeneous and the border appears sharp. Figures 1 (b), (c), and (d) are optical images that show the same sample 2, 4, and 6 weeks, respectively, after exposure to ambient air at 100% RH and RT. In these images, the sample develops several regions of light optical contrast, indicated by the arrows, which have been previously shown to result from degradation [7].
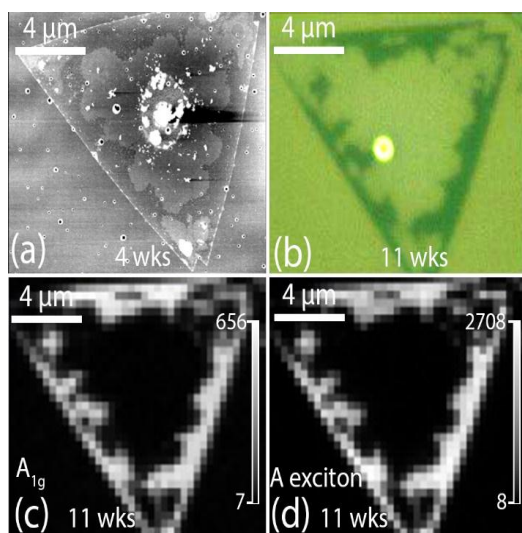

Figure 2 (a) AFM image of the sample in Figure 1 after 4 weeks in ambient air at 100% RH. (b) Optical image of the sample after 11 weeks in 100% RH. (c) and (d) Maps of A_{1g} and A exciton peak intensities, respectively, of the sample after 11 weeks in 100% RH.

To study this sample further, we carried out AFM and Raman imaging. Figure 2 (a) shows an AFM image of the sample after 4 weeks of exposure. The areas of light optical contrast observed in Figure 1 correspond with higher elevations in the AFM image. In Ref. [7], it was reported that such elevated regions in the AFM images correspond with regions containing dendritic structures and are indicative of degradation. We also carried out Raman and PL mapping of the sample after 11 weeks of exposure. Figure 2 (b) shows an optical image of the sample after 11 weeks, and Figures 2 (c) and (d) show intensity maps of the A_{1g} Raman peak and the A exciton PL peak, respectively. The regions that are degraded have significantly less Raman and PL intensity. This is consistent with previous reports of degraded ML MoS_2 [2-7]. The degradation shown in Figure 1 (d) after 6 weeks involves almost the entire sample, in contrast to the approximately 10% of degraded area in ML samples exposed at about 40% RH [2-7]. These results indicate that the increase of water vapor to 100% RH greatly accelerates the degradation of ML MoS_2. This is consistent with the reported mechanism in which water acts to accelerate the degradation by liquefying oxides, and indicates that at 40-50% RH the degradation rate is limited by lack of water.

Given that at 40-50% RH the degradation rate appears to be limited by the amount of water on the ML, we investigated MoS_2 films grown on a hydrophobic substrate and exposed to ambient air at 50% RH. We sought to determine if the hydrophobic property of the substrate reduces the amount of water molecules diffusing on the substrate to the MoS_2 ML, resulting in a slower degradation rate. Thus, we grew, using the same CVD method, ML MoS_2 on a Si_3N_4 substrate. Si_3N_4 is more hydrophobic than SiO_2, with a water contact angle of about 63° [12], instead of 23° for SiO_2 [13].

To compare the degradation of MoS_2 grown on Si_3N_4 and SiO_2, we pre-heated samples grown on Si_3N_4 and SiO_2 at 300 °C and 285 °C, respectively, for 2h. We have previously reported that the extent of degradation under ambient exposure increases as the pre-heating temperature increases in the range 285-330 °C [7]. Thus, if the hydrophobicity of Si_3N_4 has no effect on the long-term ambient degradation, we expect the MoS_2 on Si_3N_4 to degrade at a faster rate than the MoS_2 on SiO_2. After pre-heating the samples, we then left them in the same ambient environment at 40% RH, RT and room light intensity of about 1000 Lux Figure 3 (a) shows the MoS_2 sample grown on SiO_2 immediately after pre-heating in air at 285 °C for 2h. The arrow indicates the location of a grain boundary. There are no regions of light optical contrast, indicating no observable degradation. Figure 3 (b) shows the same MoS_2 sample after 3 weeks in ambient air. Areas of reduced optical contrast are developing along the edges of the sample and along the grain boundary, indicating degradation. Figures 3 (c) and (d) show optical and AFM images, respectively, of the same sample after 8 weeks of exposure to ambient air. The dendrites have grown, and the AFM image reveals that the areas of light optical contrast are indeed elevated. We note that the etching of the grain boundary as a result of pre-heating is difficult to observe in Figure 3 (a) because the sample was pre-heated at a low temperature of 285 °C. However, as a result of ambient exposure, this grain boundary degraded, causing a region of elevated dendrites, indicated by the arrow in the AFM image shown in Figure 3 (d).
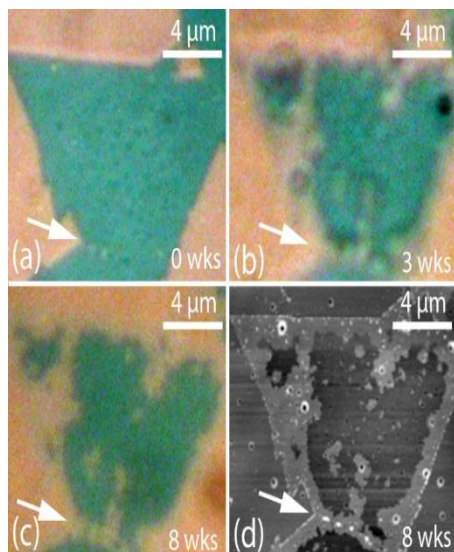
Figure 3. (a) ML MoS$_2$ sample grown on SiO$_2$ immediately after pre-heating in air at 285 ^{o}C for 2 h. (b) and (c) Optical images of the sample after 3 weeks and 8 weeks in ambient air at 40% RH, respectively. (d) AFM image corresponding to (c). The arrows indicate the location of the grain boundary.

The results for the Si$_3$N$_4$ sample are shown in Figures 4 (a) - (f). Figure 4 (a) shows a MoS$_2$ sample grown on Si$_3$N$_4$, and Figure 4 (b) shows the same sample immediately after pre-heating in air at 300 ^{o}C for 2 hours. As a result of the higher pre-heating temperature used for this sample, the grain boundaries were etched more than the sample shown in Figure 3. Consequently, wide trenches were produced, as shown by the arrow in Figure 4 (b). The AFM image in Figure 4 (f) indicates that these trenches are at a lower elevation. The sample was then left in ambient air. Figures 4 (c), (d), and (e) are optical images taken every 3 weeks of the same sample while exposed to ambient air. There are small degraded areas growing in from the edges, as indicated by the arrows. The AFM image in Figure 4 (f) confirms the presence of slight raised regions on the edges of the sample and the edges of the trenches, but there is no extensive progress of degradation into the basal plane as observed for films on SiO$_2$ in Figure 3. It appears that although the ML MoS$_2$ on Si$_3$N$_4$ still degrades, it degrades at a much slower rate than MoS$_2$ grown on SiO$_2$.
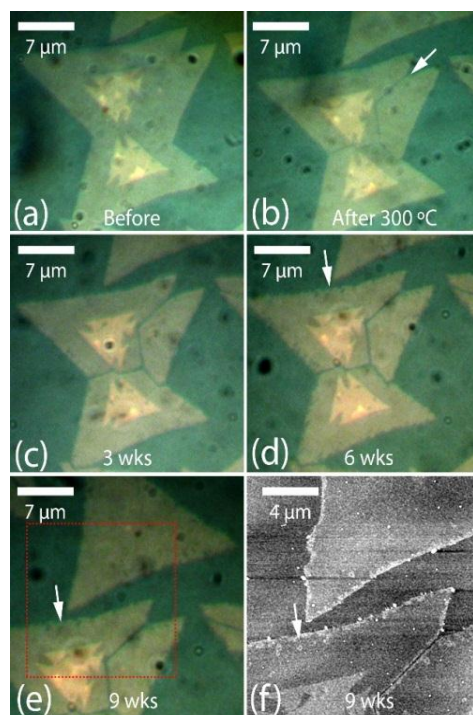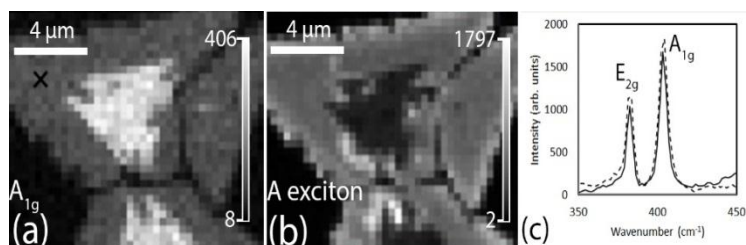
Figure 4. (a) and (b) ML MoS$_2$ sample grown on Si$_3$N$_4$ before and after pre-heating in air at 300 °C for 2 h, respectively. The arrow in (b) indicates the location of an etched grain boundary. (c), (d), and (e) Sample after 3, 6, and 9 weeks in ambient air at 40% RH, respectively. (f) AFM image corresponding to the box in (e). The arrows in (d)-(f) indicate a region of slight degradation.

To confirm that these observations do in fact indicate that MoS$_2$ grown on Si$_3$N$_4$ experiences significantly less degradation, we performed Raman and PL mapping of the sample. Figures 5 (a) and (b) show the intensity maps of the A$_{1g}$ and A exciton peaks, respectively. The intensities are remarkably uniform, indicating little to no degradation. The edges have slight inlets of lower intensities, but the basal plane shows essentially no degradation. Figure 5 (c) shows two Raman spectra after aligning the Si peaks to be at the same wavenumber, and also normalizing the spectra such that the Si peaks have the intensity. The spectrum indicated by the solid line was taken from a different freshly grown MoS$_2$ sample on SiO$_2$ (within 1 week), and the spectrum indicated by the dotted line was taken at the location indicated by the black cross in Figure 5 (a). Both of the spectra have the E$_{2g}$ peak at approximately 384 cm^{-1} and the A$_{1g}$ peak at approximately 404 cm^{-1}. The positions are consistent with the literature for pristine ML MoS$_2$, which reports the E$_{2g}$ peak at about 385 cm^{-1} and A$_{1g}$ at about 405 cm^{-1} [14]. The Raman maps of MoS$_2$ on SiO$_2$, on the other hand, have been reported to show significant decreases in intensity on the degraded ML [7]. Thus, MoS$_2$ grown on hydrophobic substrates like Si$_3$N$_4$ are less prone to degradation. It's been reported that sulfur vacancy defects in monolayer

MoS_2 cause a red shift in the E_{2g} peak of 1 to 8 cm^{-1} for sulfur vacancies of about 0.4 to 4% [16]. Between the two samples, we observe in Figure 5 (c) that the E_{2g} peak shifts less than 1 cm^{-1}, on the order of the wavenumber step size of the spectra. This provides evidence that the MoS_2 sulfur defect density of aged MoS_2 grown on Si_3N_4 that has not yet degraded is comparable to that of freshly-grown MoS_2 on SiO_2.

Figures 5 (a) and (b) show intensity maps of the A_{1g} and A exciton peaks, respectively. Figure 5 (c) shows two Raman spectra; the spectrum indicated by the dotted line was collected on this sample at the location indicated by the black cross in (a) and the spectrum indicated by the solid line was collected on a freshly grown MoS_2 sample on SiO_2.

In Refs. [17, 18], it was reported that WS_2 grown on CVD-grown graphene exhibits no signs of oxidation after at least 10 months and 300 days, respectively, of exposure to ambient air. In Ref. [17], the stability was attributed to the screening of the surface electric field by the graphene, and in Ref. [18], to charge transfer effects and the high WS_2 crystallinity resulting from growth on graphene. We note that graphene is hydrophobic, and thus its hydrophobicity may also play a role in stabilizing the TMDs.

CONCLUSIONS

We find that at an ambient RH of 40%, the degradation rate of CVD-grown ML MoS_2 appears to be limited by the amount of water on the ML. We find that CVD-grown ML MoS_2 films grown on the hydrophobic substrate Si_3N_4 degrade significantly less than films grown on the hydrophilic substrate SiO_2 when pre-heated and then exposed to ambient air at 40% RH and RT. We propose that this is due to the reduced amount of water diffusing from the substrate and onto the ML. These results show that 2D TMDs grown on hydrophobic substrates may be more resilient to degradation from ambient environments in cases in which the amount of water adsorbed on the ML is a limiting factor in the degradation rate. Future work will explore the use of other hydrophobic substrates such as HfO_2 in slowing the degradation rate.

ACKNOWLEDGMENTS

References:

[1]   Q.H. Wang, K. Kalantar-Zadeh, A. Kis, J.N. Coleman and M.S. Strano, Nat. Nanotechnol. **7**, 699 (2012).

[2]   J. Gao, B. Li, J. Tan, P. Chow, T.M. Lu and N. Koratkar, ACS Nano **10**, 2628 (2016).

[3]   H. Şar, A. Özden, İ. Demiroğlu, C. Sevik, N.K. Perkgoz and F. Ay, Phys. Status Solidi, **13**, 1800687 (2019).

[4]   J.C. Kotsakidis, Q. Zhang, A.L.V. de Parga, M. Currie, K. Helmerson, D.K. Gaskill and M.S. Fuhrer, Nano Lett. **19**, 5205 (2019).

[5]   P. Budania, P. Baine, J. Montgomery, C. McGeough, T. Cafolla, M. Modreanu, D. McNeill, N. Mitchell, G. Hughes and P. Hurley, MRS Commun. **7**, 813 (2017).

[6]   P. Afanasiev and C. Lorentz, J. Phys. Chem. C **123**, 7486 (2019).

[7]   K. Yao, J.D. Femi-Oyetoro, S. Yao, Y. Jiang, L. El Bouanani, D.C. Jones, P.A. Ecton, U. Philipose, M. El Bouanani, B. Rout and A. Neogi, 2d Mater. **7**, 015024 (2019).

[8]   Y. Cao, A. Mishchenko, G.L. Yu, E. Khestanova, A.P. Rooney, E. Prestat, A.V. Kretinin, P. Blake, M.B. Shalom, C. Woods and J. Chapman, Nano Lett., **15**, 4914 (2015).

[9]   A. Favron, E. Gaufrès, F. Fossard, A.L. Phaneuf-L'Heureux, N.Y. Tang, P.L. Lévesque, A. Loiseau, R. Leonelli, S. Francoeur and R. Martel, Nat. Mat., **14**, 826 (2015).

[10]   Y. Jiang, Y. Lin, J. Cui and U. Philipose, J. Nanomat, **2018**, 6192532 (2018).

[11]   MTI Corp. Available at: https://www.mtixtl.com/S3N4-film-1.aspx (accessed 26 March 2020).

[12]   L. Barhoumi, A. Baraket, N.M. Nooredeen, M.B. Ali, M.N. Abbas, J. Bausells and A. Errachid, Electroanal. **29**, 1586 (2017).

[13]   X. Zhan, Y. Yan, Q. Zhang and F. Chen, J. Mater. Chem. A **2**, 9390 (2014).

[14]   B. Mukherjee, F. Tseng, D. Gunlycke, K.K Amara, G. Eda and E. Simsek, Opt. Mater. Express **5**, 447 (2015).

[15]   M. Yamamoto, T.L. Einstein, M.S. Fuhrer and W.G. Cullen, J. Phys. Chem, **117**, 25643-25649 (2013)

[16]   W.M. Parkin, A. Balan, L. Liang, P.M. Das, M. Lamparski, C.H. Naylor, J.A. Rodríguez-Manzo, A.C. Johnson, V. Meunier and M. Drndic, ACS Nano, **10**, 4134-4142 (2016).

[17]   K. Kang, K. Godin, Y.D. Kim, S. Fu, W. Cha, J. Hone and E.H. Yang, Adv. Mater., **29**, 1603898 (2017).

[18]   S.Y. Kim, J. Kwak, J.H. Kim, J.U. Lee, Y. Jo, S.Y. Kim, H. Cheong, Z. Lee and S.Y. Kwon, 2d Mater., **4**, 011007 (2016).